Chemical Science

Accepted Manuscript

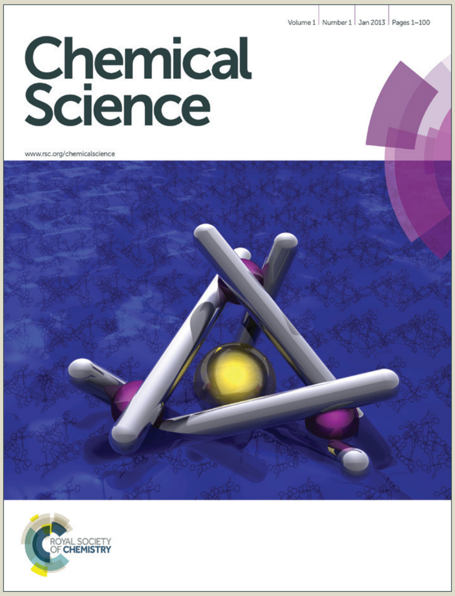

ROYAL SOCIETY OF CHEMISTRY

www.rsc.org/chemicalscience

Journal Name

RSCPublishing

ARTICLE

Cite this: DOI: 10.1039/x0xx00000x

Received 00th January 2012,
Accepted 00th January 2012

DOI: 10.1039/x0xx00000x

www.rsc.org/

Magnitude and consequence of OR ligand σ-donation on alkene metathesis activity in d^0 silica supported (≡SiO)W(NAr)(=CHtBu)(OR) catalysts

V. Mougel,[a] and C. Copéret*[a]

Well-defined silica supported W catalysts of general formula [(≡SiO)W(NAr)(=CHtBu)(OR)] (OR = $OtBu_{F9}$, $OtBu_{F6}$, $OtBu_{F3}$, OtBu and $OSi(OtBu)_3$), prepared by grafting *bis*-alkoxide complexes $[W(NAr)(=CHtBu)(OR)_2]$ on silica dehydroxylated at 700°C ($SiO_{2-(700)}$), display unexpected high activity by comparison with their Mo homologues. In this series, the activity in the self-metathesis of *cis*-4-nonene increases as a function of the OR ligand as follows: OtBu < $OtBu_{F3}$ < $OSi(OtBu)_3$ < $OtBu_{F6}$ < $OtBu_{F9}$. In addition, the ratio of the two parent metallacyclobutane intermediates, trigonal bipyramidal (TBP) / square pyramidal (SP), formed by metathesis of ethylene and observed by solid-state NMR, follows the same order: OtBu < $OtBu_{F3}$ < $OSi(OtBu)_3$ < $OtBu_{F6}$ < $OtBu_{F9}$, clearly evidencing the decreasing σ-donating ability of the OR ligand with increasing number of fluorine atoms and positioning a siloxy ligand in between $OtBu_{F3}$ and $OtBu_{F6}$. This study provides the first detailed structure-activity relationship for a series of well-defined heterogeneous catalysts showing that weaker σ-donor OR ligands lead to higher activity and that the surface siloxy ligand is overall a rather small and weak σ-donor ligand, thus providing highly active and yet stable catalysts.

Introduction

The past 50 years have witnessed extensive alkene metathesis research in both academia and industry that has resulted in numerous chemical processes and applications. While the current petrochemical processes rely on heterogeneous catalysts based on supported transition metal oxides,[1, 2] the recent development of homogeneous catalysts based on well-defined Mo, W, Re and Ru alkylidenes has led to flourishing applications in the areas of polymers and fine chemicals.[3-6] The most recent outcome even allows carrying out *Z*-selective metathesis, a major milestone for the use of metathesis towards the synthesis of advanced intermediates and complex molecules.[7-13] Furthermore, the Mo- and W-based homogeneous catalysts, when combined with Ir-dehydrogenation catalysts,[14-16] allows the upgrade of low molecular weight alkanes into high-grade diesel fuel via a tandem alkane metathesis process, as an alternative to the single component system.[17-24] All these recent applications have emerged from the rational development of homogeneous catalysts through structure – activity relationships over the past 40 years. One would thus expect that a better understanding of the reaction mechanism and of the life cycle of the corresponding heterogeneous catalysts would be a key step towards an improvement of their performances (activity, selectivity and stability).

The mechanism for alkene metathesis, proposed by Chauvin, involves the [2+2] cycloaddition of an alkene and a metal carbene to afford a metallacyclobutane intermediate.[25, 26] The metallacyclobutane then undergoes cycloreversion to either release the original reagents (degenerate) or a new alkene/alkylidene (productive). In Schrock-type catalysts of the general formula [M(NR)(=CHR)(X)(Y)] (M = Mo, W), the anionic X and Y substituents have tremendous influence on the stability of the reaction intermediates, the catalytic activity[27-29] and the stereoselectivity.[7, 30-32] A metal alkylidene complex containing X and Y ligands of notable different electron donating abilities (good and poor) facilitates the coordination of the incoming alkene and thereby the subsequent cycloaddition process.[33] The formation, structure and stability of the resulting metallacycles have been extensively reported for tungsten-based homogeneous catalysts[29, 34-38] and for few Mo systems.[35, 39, 40] Detailed solution NMR, X-Ray and computational studies have shown that these metallacycles can adopt either trigonal bipyramidal (TBP) or square pyramidal (SP) geometries that interconvert via a turnstile process (scheme 1).[27, 28, 36, 37]

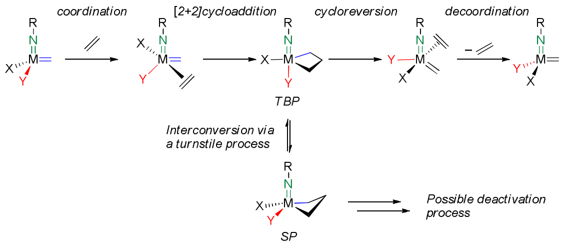

Scheme 1. Catalytic pathway proposed for d^0 alkene metathesis

DFT studies have demonstrated that the TBP isomer is on the metathesis reaction pathway and participates in the alkylidene exchange process, while the SP isomer is usually more stable and corresponds to a catalytic resting state. In addition, SP metallacycles may also be involved in deactivation processes.[41, 42]

Yet, for heterogeneous catalysts, the observation of the expected reaction intermediates, *i.e.* metallocarbenes and metallacyclobutanes, has remained a challenge, with only a single example for a well-defined silica supported tungsten catalyst.[43] In recent years, numerous well-defined supported alkylidene metathesis catalysts that exhibit similar, or in some cases greater, catalytic activity than their homogeneous analogues were developed.[22, 44-58] In particular, the controlled grafting of well-defined Mo and W precursors on silica partially dehydroxylated at 700°C ($SiO_{2-(700)}$) provides "single-site" silica-supported systems, where site isolation prevents binuclear decomposition thus increasing the stability of the catalyst.[56, 57] The resulting silica-supported alkylidene complexes [(≡SiO)M(NAr)(=CHR)(X)] lead to intrinsically dissymmetric metal centers to produce highly reactive surface species. The reactivity and stability of these complexes can be tuned by varying the X-ligand. While the most active catalysts are based on M = Mo with X = pyrrolyl,[54] the hexafluoro-*tert*-butoxide (X = $OtBu_{F6}$) showed promising performance.[55] We also showed that the analogous W-imido catalysts (X = CH_2tBu and 2,5-dimethylpyrrolyl) are less active than their Mo-analogues by *ca.* one order of magnitude in the self-metathesis of propene, but display much greater stability. In fact, we exploited the stability of the W-imido species to observe for the first time the metallacyclobutane intermediates on a supported catalyst.[43] Clearly the electronic environment around the metal center plays a crucial role in the reactivity of the supported alkylidene. The quantification of σ-donation properties of the anionic X ligand is critical to the elaboration of a structure-activity relationship, but has remained elusive.

Here, we investigate a family of well-defined silica supported tungsten alkylidene alkoxide complexes obtained from grafting [W(NAr)(=CHtBu)$(OR)_2$] complexes {OR = $OC(CF_3)_3$ ($OtBu_{F9}$); $OCMe(CF_3)_2$ ($OtBu_{F6}$); $OCMe_2(CF_3)$ ($OtBu_{F3}$); OtBu; $OSi(OtBu)_3$; Ar = 2,6-$iPr_2C_6H_3$} on silica partially dehydroxylated at 700 °C, $SiO_{2-(700)}$. These supported catalysts display activities and stabilities that in most cases surpass their molecular precursors, and even the best silica-supported Mo-analogues. Evaluation of the σ-donating ability of the OR-ligands from the spectroscopically observed ratio of TBP/SP metallacycles allows us to establish a detailed structure – reactivity relationship for [(≡SiO)W(NAr)(=CHtBu)(OR)], where catalysts with weaker σ-donating OR ligands (stronger electron withdrawing) exhibit higher activity.

Results and discussion

Synthesis of molecular precursors.

The molecular precursors [W(NAr)(=CHtBu)$(OR)_2$], $\mathbf{W_{OR}}$, (OR = $OtBu_{F6}$, O-tBu) were synthesized by salt metathesis from the bis-triflate complex [W(NAr)(=CHtBu)$(OTf)_2$(DME)] and lithium alkoxides as previously described.[38] Note that for OR = $OtBu_{F3}$, we prepared the DME adduct [W(NAr)(=CHtBu)$(OtBu_{F3})_2$(DME)] ($\mathbf{W_{OtBuF3}}$) because it was much more stable and more convenient to use for grafting (*vide infra*). In addition, we prepared $\mathbf{W_{OtBuF9}}$ and $\mathbf{W_{OSi(OtBu)3}}$ via a similar route in 69% and 88% yield, respectively using $LiOtBu_{F9}$ and $KOSi(OtBu)_3$.[59] These two unreported compounds were characterized by NMR and elemental analysis, and the crystal structure of $\mathbf{W_{OtBuF9}}$ was resolved (see Supporting Information for details).[60]

Grafting of the molecular precursors.

Grafting [W(NAr)(=CHtBu)$(OR)_2$], (OR = $OtBu_{F9}$, $OtBu_{F6}$, OtBu, $OSi(OtBu)_3$) or [W(NAr)(=CHtBu)$(OtBu_{F3})_2$(DME)] on $SiO_{2-(700)}$ yielded the corresponding materials ($\mathbf{W_{OR}@SiO_2}$). Monitoring the grafting step by IR spectroscopy shows that the isolated surface silanols at 3747 cm^{-1} for $SiO_{2-(700)}$ disappeared while the stretching and bending (C-H) vibrations of the ligands appeared in the 3100-2800 and 1500-1350 cm^{-1} regions, respectively (Fig. S2). A broad band in the 3650 cm^{-1} was present in each material and is associated with remaining unreacted OH groups interacting with adjacent ligands. The shift of the maximum of that band to higher wavenumber with the increase of the fluorine content of the OR ligand indicates that such interaction involves the tBu ligands and the fluorine when present. W elemental analysis is consistent with partial consumption of the OH groups (0.18–0.21 mmol $W.g^{-1}$ vs. 0.26 $mmol.g^{-1}$ OH). In all cases, grafting is accompanied with the release of ROH, consistent with the formation of the expected surface complexes [(≡SiO)W(NAr)(=CHtBu)(OR)] (OR = $OtBu_{F9}$ (**1**), $OtBu_{F6}$ (**2**), $OtBu_{F3}$ (**3**), OtBu (**4**), $OSi(OtBu)_3$ (**5**) (scheme 2).

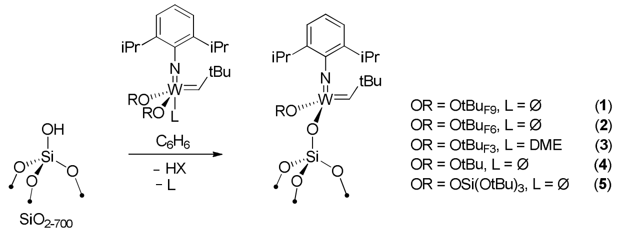

Scheme 2. Grafting of $\mathbf{W_{OR}}$ molecular complexes on $SiO_{2\text{-}(700)}$ affording $\mathbf{W_{OtBuF9}@SiO_2}$, $\mathbf{W_{OtBuF6}@SiO_2}$, $\mathbf{W_{OtBuF3}@SiO_2}$, $\mathbf{W_{OtBu}@SiO_2}$ or $\mathbf{W_{OSi(OtBu)3}@SiO_2}$. For OR = OtBu, grafting led to *ca.* 40% [(≡SiO)W(NAr)(CH_2tBu)$(OtBu)_2$] byproduct.

More specifically, grafting of $\mathbf{W_{OR}}$ (OR = $OtBu_{F9}$ and $OtBu_{F6}$) releases ca. 0.8 equiv. of HOR per surface silanol, a good evidence for **1** and **2** being formed as major surface species. For [W(NAr)(=CHtBu)$(OtBu_{F3})_2$(DME)], grafting is accompanied with the release of ca. 0.8 equiv of $HOtBu_{F3}$ and 0.9 equiv. of DME, consistent with the formation of **3** as a major species. In the case of [W(NAr)(=CHtBu)$(OtBu)_2$], only 0.4 equiv. of tBuOH is released when grafting is performed under the same conditions. This value increases to 0.6 equiv. when grafting is carried out at lower temperature (-40 °C in toluene). In this case [(≡SiO)W(NAr)(=CHtBu)(OtBu)] (**4**) is formed along with [(≡SiO)W(NAr)(CH_2tBu)$(OtBu)_2$] (ca. 30-40%) (*vide infra*), which probably results from the subsequent reaction of the released tBuOH with the surface species **4**.[43, 58, 61] For [W(NAr)(=CHtBu)$(OSi(OtBu)_3)_2$], 0.5 equiv. of $HOSi(OtBu)_3$ per surface silanol is released and a low loading is obtained upon grafting $\mathbf{W_{OSi(OtBu)3}}$ probably because of the large size of $OSi(OtBu)_3$. The compositions of $\mathbf{W_{OR}@SiO_2}$ were confirmed by elemental analysis of C, N, H and F elements (table 1).

The ^{1}H Magic Angle Spinning (MAS) NMR spectra of compounds $\mathbf{W_{OR}@SiO_2}$ (figures S3-11) displayed signals at chemical shift very close to these of the molecular precursors, in agreement with the formation of [(≡SiO)W(NAr)(=CHtBu)(OR)] as major surface species. The alkylidene W=C*H*tBu resonance is located at 8.92 ppm for **1**, 8.60 ppm for **2,** 8.29 ppm for **3**, 7.99 ppm for **4** and 8.35 ppm for **5**, respectively, following the same trend that observed for the chemical shift of the parent molecular complexes in solution (table 1). The ^{13}C cross polarisation magic angle spinning (CP MAS) solid state NMR spectra of $\mathbf{W_{OR}@SiO_2}$ (figures S4-12) are also in good agreement with the proposed structures. While a direct evidence of the alkylidene ligand by carbon-13 NMR is not possible without ^{13}C enrichment at this position,[43, 61] each material contains two sharp signals at 46.1 and 32.4 ppm for **1**, 45.2 and 32.2 ppm for **2**, 45.0 and 32.4 ppm for **3**, 44.5 and 33.0 ppm for **4** and 45.5 and 33.4 ppm for **5** assignable to the β- and γ-

Table 1. Comparative mass balance analysis and NMR chemical shift observed for the samples after grafting

Entry	*W [wt%]*[a]	*ROH$_{released}$*[b] *[RO/W$_{surf}$]*	*C [wt%]*	*C/W*[c]	*H [wt%]*	*H/W*[c]	*N [wt%]*	*N/W*[c]	*F [wt%]*	*F/W*[c]	*^{1}H$_{alkylidene}$*[d] *(ppm)*
$W_{OtBuF9}@SiO_2$	3.47 (0.19)	0.76	4.84	21.3 (21)	0.51	26.8 (27)	0.38	1.4 (1)	3.14	8.8 (9)	8.92 (9.46)
$W_{OtBuF6}@SiO_2$	3.88 (0.21)	0.80	5.39	21.3 (21)	0.65	30.6 (30)	0.37	1.3 (1)	2.05	5.1 (6)	8.60 (8.83)
$W_{OtBuF3}@SiO_2$	3.71 (0.20)	0.85	5.18	21.4 (21)	0.72	35.4 (33)	0.38	1.3 (1)	1.09	2.8 (3)	8.29 (8.38)
$W_{OtBu}@SiO_2$	3.32 (0.18)	0.60	4.78	22.0 (21)	0.68	37.4 (36)	0.48	1.9 (1)	-	-	7.99 (8.01)
$W_{OSi(OtBu)3}@SiO_2$	2.48 (0.15)	0.54	4.72	29.1 (29)	0.76	55.9 (54)	0.29	1.5 (1)	-	-	8.35 (8.19)

[a] Value in $mmol.g^{-1}$ is given in brackets. [b] Protonated form of the OR ligand released upon grafting of the precursor, quantified by ^{1}H NMR of the filtrate after grafting with internal standard. [c] The theoretical value is given in brackets. [d] Chemical shift observed for the parent molecular complex is given in brackets.

carbons of the neopentylidene group. An extra signal at 72 ppm is observed in the ^{13}C CP MAS NMR spectrum of **W_{OtBu}@SiO_2** consistent with the formation of [(≡SiO)W(NAr)(CH_2tBu)($OtBu)_2$] likely by the partial protonation of the alkylidene by *t*BuOH.[43, 61]Such signal is not observed in other supported alkylidenes, showing that if present, they correspond only to minor surface species (< 10%).

Catalytic activity.

We evaluated the catalytic activity of all the complexes in the self-metathesis of *cis*-4-nonene as a prototypical liquid substrate. All catalytic tests involved contacting the solid catalysts (0.1 mol% or 0.02 mol%) with a 0.8 M toluene solution of *cis*-4-nonene at 30 °C. All supported catalysts **W_{OR}@SiO_2** are active in metathesis in the conditions described above, resulting in the formation of 4-octenes and 5-decenes as the only products observable by GC (table 2). While thermodynamic conversion is reached for all catalysts at 0.1 mol% loading, their activity increases with an increase of the electron withdrawing character of the alkoxide ligands (OtBu < $OtBu_{F3}$ < $OtBu_{F6}$ < $OtBu_{F9}$) and places OSi$(OtBu)_3$ in between $OtBu_{F3}$ and $OtBu_{F6}$. For comparison, the catalytic activity of the molecular precursors [W(NAr)(=CHtBu)$(OR)_2$] (OR = $OtBu_{F9}$, $OtBu_{F6}$, $OtBu_{F3}$, OtBu, OSi$(OtBu)_3$) was investigated under the same reaction conditions. A similar trend is observed for OR = OtBu, $OtBu_{F3}$ and $OtBu_{F6}$ [38] but not for $OtBu_{F9}$, which falls in between $OtBu_{F3}$ and $OtBu_{F6}$ (Figure S28 and table S5).

Surprisingly, the molecular complex [W(NAr)(=CHtBu)(OSi$(OtBu)_3)_2$] is inactive (<1% conversion after 24h), despite the high activity of the grafted complex. One possible explanation of this deviation in activity between the grafted complexes and their molecular analogues is that the electron withdrawing ability of $OtBu_{F9}$ and OSi$(OtBu)_3$ ligands is compensated by their relatively larger size, as evaluated by their larger buried volume according to Cavallo's model (Table S4).[63] The lower affinity towards hydrocarbon in the case of the perfluorinated $OtBu_{F9}$ ligand[64] might also influence its reactivity by preventing the approach of the alkene and the formation of the metallacyclobutane. Note that grafting also dramatically enhanced the activity of the OtBu complex, converting a virtually inactive complex into an active catalyst as already observed for the Mo-system.[55] Noteworthy grafting on silica allowed ranking the properties of alkoxide ligand series, which was not possible on the molecular precursors due to steric constraints.

Table 2. Initial TOF and time to equilibrium of supported complexes towards self-metathesis of *cis*-4-nonene in toluene, catalysts loading 0.1 mol%, 30°C.[a]

Precursor	Silica supported		Unsupported	
	TOF_{3min}[b]	Time[c]	TOF_{3min}[b]	Time[c]
W_{OtBuF9}	115	< 10 min	93	< 10 min
W_{OtBuF6}	75	< 30 min	>166	< 3min
W_{OtBuF3}	15	< 120 min	61	24h (39%)[d]
W_{OtBu}	5	< 480 min	<1	24h (< 2%)[d]
$W_{OSi(OtBu)3}$	41	< 30 min	<1	24h (< 1%)[d]
Mo_{OtBuF6}	46	< 30 min	>166	< 3min

[a] 0.8 M solution of *cis*-4-nonene in toluene containing heptane as internal standard (0.1 M); loading in mol% was calculated based on W wt%. [b] TOF is defined here as the number of new alkenes produced per W atom and unit of time, that is without taking into account isomerization of the precursor to trans-4-nonene.[62] [c] Time to equilibrium conversion. [d] Values in parentheses are given when the system did not reach equilibrium conversion, and correspond to the measured conversion after 24h.

These silica supported tungsten arylimido alkylidene complexes are highly active alkene metathesis catalysts. In fact, it is noteworthy that **W_{OtBuF6}@SiO_2** display greater catalytic activity than the corresponding Mo complex bearing the same ligands [(≡SiO)Mo(NAr)(=CHtBu)($OtBu_{F6}$)] (Table 2). It should be noted that catalysts **W_{OtBuF9}@SiO_2** and **W_{OtBuF6}@SiO_2** readily catalyze metathesis of *cis*-4-nonene with loading as low as 0.02 mol%, reaching equilibrium in less than 3.5h for **W_{OtBuF9}@SiO_2** and 12h for **W_{OtBuF6}@SiO_2** (Table S7 and figure S30). The activity in *cis*-4-nonene metathesis at very low loading was investigated for the most active complex **W_{OtBuF9}@SiO_2**, and full conversion was obtained with catalyst loading as low as 50 ppm in 48h at 30°C.

Stability of the grafted complexes.

Dimerization of the molecular precursors during reaction has been proposed to be one of the main routes for deactivation of molecular tungsten alkylidene complexes.[65] Schrock reported that the molecular complex [W(NAr)(=CHtBu)$(OtBu_{F3})_2$] has high initial catalytic activity towards *cis*-alkenes, though this catalyst rapidly deactivates via dimerization.[15,18] We have here investigated the stability of the supported analogue $\mathbf{W_{OtBuF3}@SiO_2}$. The exposure of $\mathbf{W_{OtBuF3}@SiO_2}$ to 20 equivalents of *cis*-3-hexene in toluene for 12 h[66] prior to the catalytic test with *cis*-4-nonene did not result in any significant change in the catalytic activity of the catalyst (see supporting information for details), in sharp contrast to its molecular precursor $[W(NAr)(=CHCMe_2Ph)(OtBu_{F3})_2]$, which dimerizes under the same conditions to yield the inactive species $\{W(NAr)(OtBu_{F3})_2\}_2$[38, 67] confirming the higher stability towards bimolecular deactivation provided by site isolation on a silica surface. In fact, $\mathbf{W_{OtBuF3}@SiO_2}$ can be used and recycled more than 4 times in presence of 1000 equivalents of *cis*-4-nonene without any noticeable ageing of the catalyst (similar initial rate and time to final conversion – see ESI).

Metallacycles.

In order to obtain more insight regarding the catalyst active site, we investigated the structure of reaction intermediates by solid state NMR. The catalysts $\mathbf{W_{OR}@SiO_2}$ were exposed to 10 equiv. of ^{13}C di-labeled ethylene at -196 °C. After standing 1h at room temperature, a slight color change to red-orange was observed, and the volatiles were analyzed by GC-MS, indicating the presence of 0.7-0.8 equiv. of mono-labeled carbon-13 3,3-dimethylbutene (see ESI for details). Note that for OR = OtBu, only 0.2 equiv. of mono-labeled carbon-13 3,3-dimethylbutene were recovered, likely due to a slower kinetic. The resulting solids were evacuated under high vacuum (10^{-5} mbar) for 1.5 h and analyzed by ^1H and ^{13}C solid state NMR. While the signals of the alkylidene proton were clearly observed in the ^1H solid state NMR spectra of the supported catalyst precursors, these signals quantitatively disappeared upon exposure to ethylene, confirming the reaction of the parent alkylidene (Figures 1 a) and S12-22). Moreover, the ^{13}C CP MAS NMR of the complexes contained new peaks associated with the formation of metallacyclobutane intermediates. Noteworthy no signal attributable to methylidene species were observed in this series.[43] The signals around 100 ppm and -5 ppm correspond to the TBP metallacylobutane and the signals around 50 ppm are associated with the SP isomer. The resonances corresponding to the α and β carbon signals of the TBP metallacycle were observed only in the case of **1-3** and **5**. These systems also show the ^{13}C signals of the SP isomer while in the case of **4**, it is the only one observed (Figure 1 b-f and table 3). All these assignments were confirmed by HETCOR experiments (Figures S22-S27). The TBP/SP isomer ratio can be obtained by integration of the metallacycle signals in the ^{13}C CP MAS experiments. While CP MAS experiments is not ideal for quantitative integration of carbon signals, the same nature of the carbon species (all CH_2) allows the TBP/SP ratio to be properly estimated. In the tert-butoxide ligand series, this ratio increases with the increasing number of trifluoromethyl groups of the ligand, gradually varying from a ratio TBP/SP of 8 with OR = $OtBu_{F9}$ to *ca.* 0 for the OtBu analogue (table 3). With a TBP/SP ratio of 2.5, the $OSi(OtBu)_3$ complex lies in between its $OtBu_{F3}$ and $OtBu_{F6}$ analogues.[36]

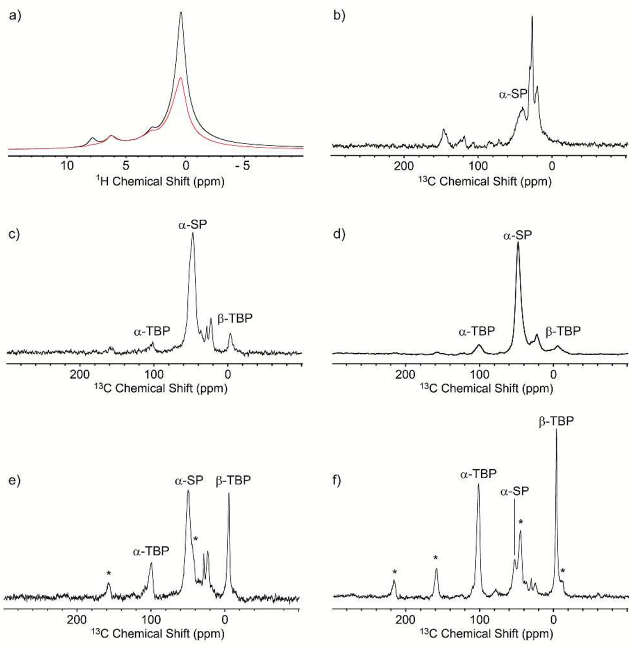

Fig. 1. ^1H MAS solid state NMR spectra of **2** before (black) and after (red) exposure to 10 equivalents of ^{13}C ethylene (a). ^{13}C CP MAS solid state NMR spectra of $\mathbf{W_{OtBu}}$ (b), $\mathbf{W_{OtBuF3}}$ (c), $\mathbf{W_{OSi(OtBu)3}}$ (d), $\mathbf{W_{OtBuF6}}$ (e) and $\mathbf{W_{OtBuF9}}$ (f) after exposure to 10 equivalents of ^{13}C ethylene. The MAS frequency was set to 10 kHz, and the contact time of the CP to 250 µs, * indicate spinning side bands.

Table 3. Solid state NMR data for the metallacyclobutane surface complexes

Compound	$\delta_{TBP}(C_\alpha)^a$	$\delta_{TBP}(C_\beta)^a$	$\delta_{SP}(C_\alpha)^a$	*Ratio TBP/SP*[b]
W_{OtBuF9}	102.6 (4.1)	-2.7 (-0.7)	50 (1.9)	83/17
W_{OtBuF6}	100.7 (4.3)	-5.4 (-0.7)	49.5 (1.6)	43/57
W_{OtBuF3}	102.3 (4.1)	-4.2 (0.0)	47.3 (1.8)	9/91
W_{OtBu}	-	-	42.5 (2.1)	0/100
$W_{OSi(OtBu)3}$	101.5 (4.2)	-6.3 (-0.1)	48.6 (1.7)	22/78

[a] Values given in ppm, determined by CP MAS experiments at 10kHz. The corresponding proton chemical shift is given in parentheses. [b] Values given in %, determined as detailed in SI.

The formation of metallacyclobutane from the five alkylidene precursors $\mathbf{W_{OR}@SiO_2}$ highlight the higher stability of the metallacycles with respect to the separated reactants in these systems, as suggested previously by theoretical studies.[28, 42] Stronger σ-donor ligands favors SP– over TBP–geometries, which could be explained by their stronger trans-influence.[68] The SP/TBP isomer ratios thus appear to be a good measure of the trans-influence of the OR-ligand (σ-donation). The SP/TBP ratios in these series of dissymmetric surface complexes decreases, following the order $tBuO^-$ > $tBu_{F3}O^-$ > $tBu_{F6}O^-$ > $tBu_{F9}O^-$, in line with decreasing σ-donating ability of each ligand. The TBP/SP ratio obtained for OR = $OSi(OtBu)_3$ allows to rank its σ-donation in between $OtBu_{F3}$ and $OtBu_{F6}$. Regarding the similarity between this ligand and isolated silanols found at the surface of $SiO_{2-(700)}$, one can assume that the position of silica in this spectroscopic series would lie at a similar position, though as previously mentioned this does not include the larger steric volume of the $OSi(OtBu)_3$ ligand that a silanol on the silica surface as discussed above. Moreover, it is noteworthy that the metathesis rates of the series of catalysts follow the same trend, making a direct connection between higher rates and less σ-donor ligands in these systems.

Catalytic activity of the metallacycles.

The catalytic activity of these metallacycles were investigated and compared to the parent alkylidene complexes. As indicated in Table S8 and figure S31, the reaction profiles all present an S-type shape: a period just after addition of *cis*-4-nonene with low TOF followed by a second period with TOF following the trend and the magnitude observed for the parent complexes at the exception of $\mathbf{W_{OtBu}@SiO_2}$. These two phases (and the initiation period in particular) show that the parent metallacycles are very stable, do not readily participate in the metathesis reaction, and only slowly undergo cycloreversion, in contrast to tri-substituted metallacyclobutanes involved in the metathesis of *cis*-4-nonene. For $\mathbf{W_{OtBu}@SiO_2}$, the SP–metallacycle does not show any significant activity towards *cis*-4-nonene, which probably results from its too high stability or its high propensity to undergo deactivation.[41] Overall, the initiation phase observed with the metallacycles suggests that the induction period is due to the slow conversion of the more stable unsubstituted metallacycles into active species, thus indicating the importance of the substitution of the metallacycles on the reaction rates.[69]

Conclusions

A series of well-defined silica-supported alkylidene alkoxide tungsten catalysts [(≡SiO)W(NAr)(=CHtBu)(OR)] (OR = $OtBu_{F9}$, $OtBu_{F6}$, $OtBu_{F3}$, OtBu, $OSi(OtBu)_3$) was prepared via Surface Organometallic Chemistry. These catalysts display catalytic performances, including rates, which can exceed these of the corresponding well-defined silica supported Mo-equivalent with $OtBu_{F6}$. The order of reactivity follows the electron withdrawing character of the alkoxide-ligands ($OtBu_{F9}$ > $OtBu_{F6}$ > $OtBu_{F3}$ > OtBu) and places the siloxy ligand ($OSi(OtBu)_3$) in between the $OtBu_{F6}$ and $OtBu_{F3}$ ligands. The increased activity of the complexes bearing $OSi(OtBu)_3$ and $OtBu_{F9}$ ligands upon grafting highlights the fact that silica act as a rather small electron withdrawing ligand. It is noteworthy that the supported catalysts, including the most reactive ones, display very good stability, typically higher than their molecular analogues, allowing their recycling and the use of very low catalyst loading down to 50 ppm. In addition, these well-defined supported systems allowed a direct observation of the metallacyclobutane intermediates in supported alkene metathesis catalysts, and the quantification of the SP/TBP ratio of the metallacyclobutane intermediates provides a way to evaluate the trans-influence (σ-donation) of the OR-ligand ($OtBu_{F9}$ < $OtBu_{F6}$ < $OSi(OtBu)_3$ < $OtBu_{F3}$ < OtBu). In this series, strong electron-withdrawing OR ligands favors TBP intermediates and affords the more active catalysts, thus establishing structure-activity relationship at the molecular level and paving the way to the more rational improvement of heterogeneous alkene metathesis catalysts.

Acknowledgements

V.M. was supported by an ETH fellowship (co-funded ETH Zürich-Marie Curie action for people, FEL-08 12-2). Dr Matthew P. Conley and Maxence Valla are thanked for helpful discussions and NMR spectroscopy assistance.

Notes and references

[a] Department of Chemistry and Applied Biosciences, Vladimir Prelog Weg 2, ETH Zürich, CH-8093 Zürich, Switzerland.

† Electronic Supplementary Information (ESI) available: Complete synthetic and catalytic procedures, crystal structure of $[W(NAr)(=CHtBu)(OtBu_{F9})_2]$, (CCDC 977064) ^1H and ^{13}C solid state NMR and IR spectra. See DOI: 10.1039/b000000x/

1. J. C. Mol, *J. Mol. Catal. A-Chem.*, 2004, **213**, 39-45.
2. K. Ivin and H. Mol, in *Olefin Metathesis and Metathesis Polymerization (2)*, eds. K. J. Ivin and J. C. Mol, Academic Press, London, 1997.
3. R. R. Schrock and A. H. Hoveyda, *Angew. Chem. Int. Ed.*, 2003, **42**, 4592-4633.
4. R. H. Grubbs, *Angew. Chem. Int. Ed.*, 2006, **45**, 3760-3765.
5. A. H. Hoveyda, S. J. Malcolmson, S. J. Meek and A. R. Zhugralin, *Angew. Chem. Int. Ed.*, 2010, **49**, 34-44.
6. S. Kress and S. Blechert, *Chem. Soc. Rev.*, 2012, **41**, 4389-4408.

7. I. Ibrahem, M. Yu, R. R. Schrock and A. H. Hoveyda, *J. Am. Chem. Soc.*, 2009, **131**, 3844-+.
8. A. J. Jiang, Y. Zhao, R. R. Schrock and A. H. Hoveyda, *J. Am. Chem. Soc.*, 2009, **131**, 16630-+.
9. S. J. Meek, R. V. O'Brien, J. Llaveria, R. R. Schrock and A. H. Hoveyda, *Nature*, 2011, **471**, 461-466.
10. D. V. Peryshkov, R. R. Schrock, M. K. Takase, P. Muller and A. H. Hoveyda, *J. Am. Chem. Soc.*, 2011, **133**, 20754-20757.
11. R. K. M. Khan, S. Torker and A. H. Hoveyda, *J. Am. Chem. Soc.*, 2013, **135**, 10258-10261.
12. K. Endo and R. H. Grubbs, *J. Am. Chem. Soc.*, 2011, **133**, 8525-8527.
13. B. K. Keitz, K. Endo, P. R. Patel, M. B. Herbert and R. H. Grubbs, *J. Am. Chem. Soc.*, 2012, **134**, 693-699.
14. A. S. Goldman, A. H. Roy, Z. Huang, R. Ahuja, W. Schinski and M. Brookhart, *Science*, 2006, **312**, 257-261.
15. B. C. Bailey, R. R. Schrock, S. Kundu, A. S. Goldman, Z. Huang and M. Brookhart, *Organometallics*, 2009, **28**, 355-360.
16. M. C. Haibach, S. Kundu, M. Brookhart and A. S. Goldman, *Acc. Chem. Res.*, 2012, **45**, 947-958.
17. V. Vidal, A. Theolier, J. ThivolleCazat and J. M. Basset, *Science*, 1997, **276**, 99-102.
18. C. Copéret, O. Maury, J. Thivolle-Cazat and J. M. Basset, *Angew. Chem. Int. Ed.*, 2001, **40**, 2331-+.
19. E. Le Roux, M. Chabanas, A. Baudouin, A. de Mallmann, C. Copéret, E. A. Quadrelli, J. Thivolle-Cazat, J. M. Basset, W. Lukens, A. Lesage, L. Emsley and G. J. Sunley, *J. Am. Chem. Soc.*, 2004, **126**, 13391-13399.
20. E. Le Roux, M. Taoufik, C. Copéret, A. de Mallmann, J. Thivolle-Cazat, J. M. Basset, B. M. Maunders and G. J. Sunley, *Angew. Chem. Int. Ed.*, 2005, **44**, 6755-6758.
21. F. Blanc, C. Copéret, J. Thivolle-Cazat and J.-M. Basset, *Angewandte Chemie International Edition*, 2006, **45**, 6201-6203.
22. F. Blanc, J. Thivolle-Cazat, J. M. Basset and C. Copéret, *Chem. Eur. J.*, 2008, **14**, 9030-9037.
23. J.-M. Basset, C. Copéret, D. Soulivong, M. Taoufik and J. T. Cazat, *Acc. Chem. Res.*, 2010, **43**, 323-334.
24. C. Copéret, *Chem. Rev.*, 2009, **110**, 656-680.
25. Y. Chauvin, *Angew. Chem. Int. Ed.*, 2006, **45**, 3740-3747.
26. J. L. Herisson and Y. Chauvin, *Makromolekulare Chemie*, 1971, **141**, 161-&.
27. A. Poater, X. Solans-Monfort, E. Clot, C. Copéret and O. Eisenstein, *J. Am. Chem. Soc.*, 2007, **129**, 8207-8216.
28. X. Solans-Monfort, C. Copéret and O. Eisenstein, *Organometallics*, 2012, **31**, 6812-6822.
29. J. Feldman, R. T. Depue, C. J. Schaverien, W. M. Davis and R. R. Schrock, *Advances in Metal Carbene Chemistry*, 1989.
30. S. J. Malcolmson, S. J. Meek, E. S. Sattely, R. R. Schrock and A. H. Hoveyda, *Nature*, 2008, **456**, 933-937.
31. S. C. Marinescu, D. S. Levine, Y. Zhao, R. R. Schrock and A. H. Hoveyda, *J. Am. Chem. Soc.*, 2011, **133**, 11512-11514.
32. S. C. Marinescu, R. R. Schrock, P. Muller, M. K. Takase and A. H. Hoveyda, *Organometallics*, 2011, **30**, 1780-1782.
33. X. Solans-Monfort, E. Clot, C. Copéret and O. Eisenstein, *J. Am. Chem. Soc.*, 2005, **127**, 14015-14025.
34. J. Feldman and R. R. Schrock, *Progress in Inorganic Chemistry*, 1991, **39**, 1-74.
35. R. R. Schrock, A. J. Jiang, S. C. Marinescu, J. H. Simpson and P. Muller, *Organometallics*, 2010, **29**, 5241-5251.
36. J. Feldman, W. M. Davis and R. R. Schrock, *Organometallics*, 1989, **8**, 2266-2268.
37. J. Feldman, W. M. Davis, J. K. Thomas and R. R. Schrock, *Organometallics*, 1990, **9**, 2535-2548.
38. R. R. Schrock, R. T. Depue, J. Feldman, K. B. Yap, D. C. Yang, W. M. Davis, L. Park, M. Dimare, M. Schofield, J. Anhaus, E. Walborsky, E. Evitt, C. Kruger and P. Betz, *Organometallics*, 1990, **9**, 2262-2275.
39. R. R. Schrock, J. S. Murdzek, G. C. Bazan, J. Robbins, M. Dimare and M. Oregan, *J. Am. Chem. Soc.*, 1990, **112**, 3875-3886.
40. G. C. Bazan, R. R. Schrock and M. B. Oregan, *Organometallics*, 1991, **10**, 1062-1067.
41. A. M. Leduc, A. Salameh, D. Soulivong, M. Chabanas, J. M. Basset, C. Copéret, X. Solans-Monfort, E. Clot, O. Eisenstein, V. P. W. Bohm and M. Roper, *J. Am. Chem. Soc.*, 2008, **130**, 6288-6297.
42. X. Solans-Monfort, C. Copéret and O. Eisenstein, *J. Am. Chem. Soc.*, 2010, **132**, 7750-7757.
43. F. Blanc, R. Berthoud, C. Copéret, A. Lesage, L. Emsley, R. Singh, T. Kreickmann and R. R. Schrock, *Proc. Nat. Acad. Sci. U.S.A.*, 2008, **105**, 12123-12127.
44. W. A. Herrmann, A. W. Stumpf, T. Priermeier, S. Bogdanovic, V. Dufaud and J. M. Basset, *Angew. Chem. Int. Ed.*, 1996, **35**, 2803-2805.
45. F. Blanc, M. Chabanas, C. Copéret, B. Fenet and E. Herdweck, *J. Organomet. Chem.*, 2005, **690**, 5014-5026.
46. S. I. Wolke and R. Buffon, *J. Mol. Catal. A-Chem.*, 2000, **160**, 181-187.
47. M. Chabanas, A. Baudouin, C. Copéret and J. M. Basset, *J. Am. Chem. Soc.*, 2001, **123**, 2062-2063.
48. M. Chabanas, A. Baudouin, C. Copéret, J.-M. Basset, W. Lukens, A. Lesage, S. Hediger and L. Emsley, *J. Am. Chem. Soc.*, 2003, **125**, 492-504.
49. M. Chabanas, C. Copéret and J.-M. Basset, *Chemistry – A European Journal*, 2003, **9**, 971-975.
50. H. Balcar, N. Zilkova, J. Sedlacek and J. Zednik, *J. Mol. Catal. A-Chem.*, 2005, **232**, 53-58.
51. F. Blanc, C. Copéret, J. Thivolle-Cazat, J. M. Basset, A. Lesage, L. Emsley, A. Sinha and R. R. Schrock, *Angew. Chem. Int. Ed.*, 2006, **45**, 1216-1220.
52. B. Rhers, A. Salameh, A. Baudouin, E. A. Quadrelli, M. Taoufik, C. Copéret, F. Lefebvre, J. M. Basset, X. Solans-Monfort, O. Eisenstein,

W. W. Lukens, L. P. H. Lopez, A. Sinha and R. R. Schrock, *Organometallics*, 2006, **25**, 3554-3557.

53. F. Blanc, R. Berthoud, A. Salameh, J. M. Basset, C. Copéret, R. Singh and R. R. Schrock, *J. Am. Chem. Soc.*, 2007, **129**, 8434-+.
54. F. Blanc, J. Thivolle-Cazat, J. M. Basset, C. Copéret, A. S. Hock, Z. J. Tonzetich and R. R. Schrock, *J. Am. Chem. Soc.*, 2007, **129**, 1044-1045.
55. N. Rendon, R. Berthoud, F. Blanc, D. Gajan, T. Maishal, J. M. Basset, C. Copéret, A. Lesage, L. Emsley, S. C. Marinescu, R. Singh and R. R. Schrock, *Chem. Eur. J.*, 2009, **15**, 5083-5089.
56. C. Copéret, *Dalton Trans.*, 2007, 5498-5504.
57. N. Rendon, F. Blanc and C. Copéret, *Coord. Chem. Rev.*, 2009, **253**, 2015-2020.
58. D. Gajan, N. Rendon, K. M. Wampler, J. M. Basset, C. Copéret, A. Lesage, L. Emsley and R. R. Schrock, *Dalton Trans.*, 2010, **39**, 8547-8551.
59. It should be noted that the synthesis of the neophylidene analogue of $WOtBuF_9$ $[W(NAr)(CHMe_2Ph)(OtBuF_9)_2]$ was recently described) in ref. 15
60. The overall geometry of $WOtBuF_9$ is pseudotetrahedral with a syn-alkylidene, two symmetric alkoxides and a linear imido ligand, similarly to the previously described crystal structures of its WOR analogues (OR = $OtBuF_6$, $OtBuF_3$ and OtBu), with a W=C bond of 1.870(8) Å, in the range of previously described W-carbene bond (Fig. S1, Tables S1-3).
61. M. P. Conley, V. Mougel, D. V. Peryshkov, W. P. Forrest, D. Gajan, A. Lesage, L. Emsley, C. Copéret and R. R. Schrock, *J. Am. Chem. Soc.*, 2013, **135**, 19068-19070.
62. J. L. Bilhou, J. M. Basset, R. Mutin and W. F. Graydon, *J. Am. Chem. Soc.*, 1977, **99**, 4083-4090.
63. https://www.molnac.unisa.it/OMtools/sambvca.php
64. D. O'Hagan, *Chem. Soc. Rev.*, 2008, **37**, 308-319.
65. A. K. Rappe and W. A. Goddard, *J. Am. Chem. Soc.*, 1982, **104**, 448-456.
66. Conditions used in ref. 67 for the quantitative dimerization of the molecular precursor $WOtBuF_3$
67. L. P. H. Lopez, R. R. Schrock and P. Muller, *Organometallics*, 2006, **25**, 1978-1986.
68. B. J. Coe and S. J. Glenwright, *Coord. Chem. Rev.*, 2000, **203**, 5-80.
69. C. Wang, F. Haeffner, R. R. Schrock and A. H. Hoveyda, *Angew. Chem. Int. Ed.*, 2013, **52**, 1939-1943.